Observation of Complex Bound States in the Spin-1/2 Heisenberg XXZ Chain Using Local Quantum Quenches

Martin Ganahl,[1] Elias Rabel,[1,2] Fabian H. L. Essler,[3] and H. G. Evertz[1,*]

[1]*Institut für Theoretische Physik, Technische Universität Graz, Petersgasse 16, 8010 Graz, Austria*
[2]*Institut für Festkörperforschung, Forschungszentrum Jülich, 52425 Jülich, Germany*
[3]*The Rudolf Peierls Centre for Theoretical Physics, Oxford University, Oxford OX1 3NP, United Kingdom*

(Received 20 December 2011; published 17 February 2012)

We consider the nonequilibrium evolution in the spin-1/2 XXZ Heisenberg chain for fixed magnetization after a local quantum quench. This model is equivalent to interacting spinless fermions. Initially an infinite magnetic field is applied to n consecutive sites and the ground state is calculated. At time $t = 0$ the field is switched off and the time evolution of observables such as the z component of spin is computed using the time evolving block decimation algorithm. We find that the observables exhibit strong signatures of linearly propagating spinon and bound state excitations. These persist even when integrability-breaking perturbations are included. Since bound states (''strings'') are notoriously difficult to observe using conventional probes such as inelastic neutron scattering, we conclude that local quantum quenches are an ideal setting for studying their properties. We comment on implications of our results for cold atom experiments.

DOI: 10.1103/PhysRevLett.108.077206 PACS numbers: 75.10.Pq, 02.30.Ik, 05.60.Gg, 67.85.−d

Cold atomic gases provide an ideal testing ground for nonequilibrium many-body quantum physics because the dynamics remain coherent for long times by virtue of the weak coupling to the environment. Recent experiments [1,2] have opened up the study of an entirely new regime in many particle quantum physics. The ''quantum Newton's cradle'' experiments of Kinoshita *et al.* drew attention to the importance of dimensionality and conservation laws and prompted a huge number of theoretical analyses on the role played by quantum integrability [3,4]. A standard protocol for driving a quantum system out of equilibrium is by means of a quantum quench (QQ): a system is prepared in the ground state of a given Hamiltonian H_0. At time $t = 0$ an experimentally tunable parameter that characterizes the Hamiltonian (e.g., a magnetic field) is changed suddenly and one then considers the unitary time evolution of the system by means of the new Hamiltonian H. QQs can be either global or local and we focus on the latter case in the following. A particular case of a local QQ is given by the x-ray edge singularity, which is a central paradigm of many-body physics. The types of problems we consider below can be viewed as generalizations of x-ray edge problems, the most crucial difference arising from the initial state and the kind of observable that we consider, which can be measured, e.g., in realizations based on cold atomic gases.

We consider the anisotropic spin-1/2 Heisenberg chain on a lattice with N sites with fixed numbers $N_{\uparrow,\downarrow}$ of up and down spins and open boundary conditions [5])

$$H(\Delta, B_0) = J \sum_{i=1}^{N-1} S_i^x S_{i+1}^x + S_i^y S_{i+1}^y + \Delta S_i^z S_{i+1}^z - B_0(t) \sum_{i=i_0}^{i_0+m_0-1} S_i^z, \qquad (1)$$

where $J > 0$ and B_0 is a local magnetic field acting on m_0 consecutive sites starting at position i_0. It is well known that (1) can be mapped to a model of spinless fermions with nearest-neighbor density-density interaction by means of a Jordan-Wigner transformation, and all of our results are straightforwardly translated into that setting. The study of local QQs in models of the kind (1) was initiated in 1970 [6], where the noninteracting case $\Delta = 0$, $m_0 = 1$ was shown to lead to a nonthermal stationary state. With the advent of efficient numerical approaches [7,8], local quenches in the interacting XXZ chain [9,10] and corresponding conformal field theories [11] have been studied intensely. In this Letter we show that longer quenches $m_0 > 1$ lead to prominent linearly propagating bound states, which in standard condensed matter scenarios have been difficult to discern [10,12].

We consider the following quench protocol: we prepare the system in the ground state $|0\rangle$ of the Hamiltonian $H(\Delta, B_0 = -\infty)$. At time $t = 0$ we suddenly switch off the magnetic field B_0 and then consider the time evolution, governed by the Hamiltonian $H(\Delta, B_0 = 0)$, of the following observables

$$\begin{aligned} \langle S^z \rangle(j,t) &\equiv \langle 0|S_j^z(t)|0\rangle, \\ P_{\uparrow\uparrow}(j,t) &\equiv \langle 0|P_j(t)P_{j+1}(t)|0\rangle, \\ P_{\uparrow\uparrow\uparrow}(j,t) &\equiv \langle 0|P_{j-1}(t)P_j(t)P_{j+1}(t)|0\rangle, \end{aligned} \qquad (2)$$

where $P_j = S_j^z + 1/2$ is the up-spin projection operator on site j. In the thermodynamic limit there are different regimes: when the magnetization per site m is equal to $-1/2$ the ground state of $H(\Delta, B_0 = 0)$ is given by the saturated ferromagnetic state with all spins down, and a local quench of the type described above then reduces to a quantum mechanical few-body problem. On the other

hand, for magnetizations $-1/2 < m < 0$ the model $H(\Delta, B_0 = 0)$ describes a quantum critical (Luttinger liquid) phase and our local quantum quench involves complex many-body effects and can be thought of as a generalization of the x-ray edge problem. In the following we first consider the simpler, spin-polarized case as this allows us to establish the role played by bound states.

Spin-polarized case.—In this case the ground state of $H(\Delta, 0)$ is the ferromagnetic state with all spins down $|\downarrow\rangle$. Excitations with $N_\uparrow$ spin flips (particles) can be constructed by the Bethe ansatz and are parametrized by $N_\uparrow$ momenta k_j

$$|N_\uparrow, \mathbf{k}\rangle = \sum_{x_1<\cdots<x_{N_\uparrow}} \Psi(\{k_j\}|\{x_l\}) \prod_{n=1}^{N_\uparrow} S^+_{x_n}|\downarrow\rangle. \quad (3)$$

Here the wave function Ψ has the characteristic Bethe ansatz form and the momenta $\{k_j\}$ are subject to quantization conditions, which for a ring geometry read

$$e^{iNk_j} = \prod_{\substack{l=1\\ l\neq j}}^{N_\uparrow} -\frac{2\Delta e^{ik_j} - 1 - e^{ik_j+ik_l}}{2\Delta e^{ik_l} - 1 - e^{ik_j+ik_l}}, \qquad j = 1, \ldots, N_\uparrow. \quad (4)$$

Energy and momentum are $E = \sum_{j=1}^{N_\uparrow} \epsilon(k_j)$ and $P = \sum_{j=1}^{N_\uparrow} k_j$, respectively, where $\epsilon(k) = J(\cos k - \Delta)$. The solutions k_j of (4) can be either real or complex [13]. The former describe scattering states of "magnons," while the latter correspond to bound states. Bound states involving ℓ particles are known as "ℓ-strings" and have wave functions that exhibit exponential decay (which can be slow) with respect to the distances between particles. Their dispersion relations in the thermodynamic limit are [13,14] $\epsilon_\ell(k) = -J\frac{\sin(\nu)}{\sin(\ell\nu)}[\cos(\ell\nu) - (-1)^\ell \cos(k)]$, where $\Delta = \cos(\nu)$. Here the total momentum k of ℓ-strings is constrained, e.g., for $|\Delta| < 1$ and $\ell = 2$ we have $|k| > 2\nu$. For a given value of Δ there generally exists a hierarchy of allowed strings, which was first identified in a seminal work by Takahashi and Suzuki [13]. We note that the energy difference between bound states and scattering continua can generally be very small. Using the exact eigenstates of $H(\Delta, 0)$ we can derive a Lehmann representation for the observables (2) after our quench

$$\langle\mathcal{O}\rangle(j,t) = \sum_{\{k_l\},\{p_r\}} \langle 0|m_0, \mathbf{k}\rangle\langle m_0, \mathbf{k}|\mathcal{O}_1|m_0, \mathbf{p}\rangle\langle m_0, \mathbf{p}|0\rangle \times e^{-i\sum_{n=1}^{m_0} t[\epsilon(p_n)-\epsilon(k_n)]-(j-1)[p_n-k_n]}, \quad (5)$$

where the sums are over all Bethe ansatz states with m_0 momenta. In the case $m_0 = 1$ an elementary calculation gives $\langle S^z\rangle(j,t) = -\frac{1}{2} + J^2_{j-1}(Jt)$, where J_n is a Bessel function. For large, fixed j this increases exponentially for $Jt \lesssim j$, shows a maximum for $Jt \approx j$, and exhibits an oscillatory power-law decay for $Jt \gtrsim j$. A stationary phase approximation shows that the dominant contribution in the Lehmann representation (5) for $Jt \approx j$ arises from states with $k \approx \frac{\pi}{2}, \frac{3\pi}{2}$, which propagate with the highest possible velocity $v_{\max} = \max_k|\frac{\epsilon(k)}{dk}| = J$. The fact that $\langle S^z\rangle(j,t)$ has a maximum at $Jt \approx j$ can be understood qualitatively by noting that the density of states $\rho_1(v) = \int \delta(v - d\epsilon/dk)dk = \frac{N}{2\pi}\frac{1}{\sqrt{J^2-v^2}}$ has singularities at the maximum speed $v = \pm J$. The exponential suppression of $\langle S^z\rangle(j,t)$ for $t \lesssim (j/v_{\max})$ gives rise to a horizon effect and is described by the Lieb-Robinson bound [15].

In all other cases $m_0 > 1$, string states $\ell \geq 2$ will contribute to the time evolution of observables, and in order to study their influence we have carried out numerical computations using the time evolving block decimation (TEBD) algorithm [7]. Results for $m_0 = 3$ (three neighboring sites with spin-up in the initial state) are shown in Fig. 1. As a function of the anisotropy Δ we observe three distinct regimes, which are fully consistent with expectations from the Bethe ansatz. (i) For small values of Δ we observe a single wave front in $\langle S^z\rangle(x,t)$, propagating with the maximal magnon velocity $v = J$ (the $m_0 = 1$ case discussed above looks quite similar). (ii) At $\Delta = 0.8$, a second, slower branch of propagating wave packets emerges both in $\langle S^z\rangle(x,t)$ and in $P_{\uparrow\uparrow}(x,t)$ [16]. Its propagation velocity is equal to the maximal 2-string velocity. We have verified by direct evaluation of (5) that the second front is associated with 2-strings. Interestingly there is a threshold in Δ for observing this phenomenon ($\Delta_c \approx \Delta_0 = 1/\sqrt{2}$), while 2-strings exist at any $\Delta \neq 0$. The reason is that the maximal 2-string velocity is

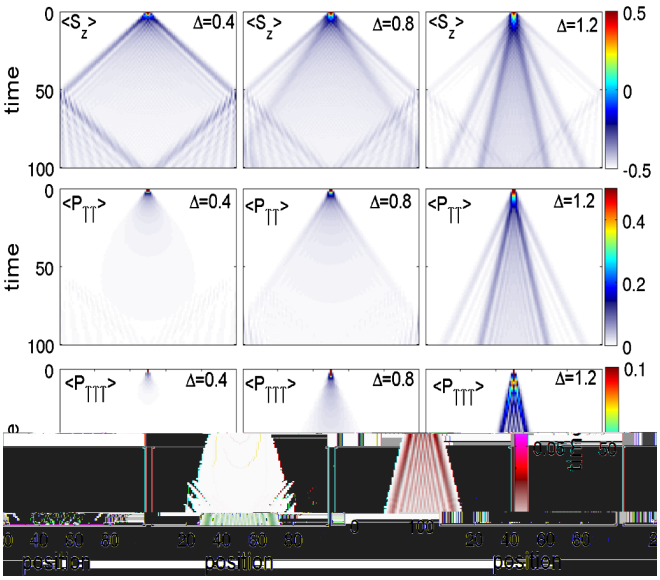

FIG. 1 (color online). Time evolution in the spin-polarized case after preparing the system in an initial state with three spin flips in the center of a 101 site chain for different values of Δ. Top row: Spacetime plot of $\langle S^z\rangle(x,t)$; middle row: $\langle\mathcal{P}_{\uparrow\uparrow}\rangle(x,t)$, which projects a bond onto $|\uparrow\uparrow\rangle\langle\uparrow\uparrow|$; bottom row: $\langle\mathcal{P}_{\uparrow\uparrow\uparrow}\rangle(x,t)$, which projects three adjacent sites onto $|\uparrow\uparrow\uparrow\rangle\langle\uparrow\uparrow\uparrow|$.

$v_{\max,2} = J\sqrt{1-\Delta^2}$ for $0 < \Delta < \Delta_0$ and $v_{\max,2} = \frac{J}{2\Delta}$ for $\Delta_0 < \Delta < 1$. On the other hand, the density of states for 2-strings is $\rho_2(v) = 2\Delta/\sqrt{J^2 - (2\Delta v)^2}$, which acquires a singularity only if $\Delta > 1/\sqrt{2}$. It is this singularity which induces a clear signature of propagating 2-strings in both $\langle S^z\rangle(x,t)$ and $P_{\uparrow\uparrow}(x,t)$. (iii) For interaction strengths above $\Delta_{c2} \approx 0.9$ we observe an additional branch in $\langle S^z\rangle(x,t)$, $P_{\uparrow\uparrow}(x,t)$, and in $P_{\uparrow\uparrow\uparrow}(x,t)$. This feature clearly arises from propagating 3-strings and can be understood in complete analogy with the 2-string case discussed above.

Results for finite magnetizations.—Here the bulk of our system is in a strongly correlated quantum critical Luttinger liquid phase and our quench protocol described above is closely related to the x-ray edge singularity problem in a correlated host [17]. However, the observables relevant to our case are different and cannot be described using methods of boundary conformal field theory [18]. We computed the quenched ground state using the density matrix renormalization group algorithm [19] and the time evolution using the TEBD with matrix dimensions up to 1200. In Fig. 2 we present results for $\Delta = 1.2$ and three different magnetizations per site $m = (N_\uparrow - N_\downarrow)/2N = -0.44, -0.26, -0.14$, corresponding to $N_\uparrow = 6, 24, 36$ on a $N = 100$ site chain. We note that this corresponds to the Luttinger liquid phase of the Heisenberg model even though $\Delta > 1$. In all cases we observe two propagating wave fronts (in each direction) in $\langle S^z\rangle(x,t)$. The results for $P_{\uparrow\uparrow}(x,t)$ show that the slower front is associated with excitations that favor neighboring spin flips. In order to interpret these results we follow our analysis of the spin-polarized case. It is known from the Bethe ansatz solution that the elementary excitations of the Heisenberg chain at finite magnetization are gapless "spinons" as well as gapped bound states associated with string solutions of the Bethe ansatz equations (4). It is then tempting to associate the faster or slower wave fronts with spinon and 2-string excitations, respectively, because, just like in the spin-polarized case, the latter induce an enhancement in the density of neighboring spin flips as a result of their bound nature. In order to substantiate this expectation we have evaluated the maximal velocities of both spinon and string excitations as functions of the magnetization per site. In Fig. 3 we present a comparison of these velocities with the ones extracted from the TEBD results in Fig. 2. We see that the results are in excellent agreement.

For magnetizations closer to zero the 2-string branch gets more and more washed out, because the momentum range of 2-string excitations diminishes and eventually vanishes as the magnetization approaches zero [13]. In order to determine whether longer strings also lead to easily recognizable features in observables after a local quench, we have analyzed the case $m_0 = 3$ for $\Delta = 1.2$ and magnetization per site $m = -0.2525$. Some results for $\langle S^z\rangle(x,t)$ are shown in Fig. 4. We can now identify three branches. The propagation velocities extracted from the

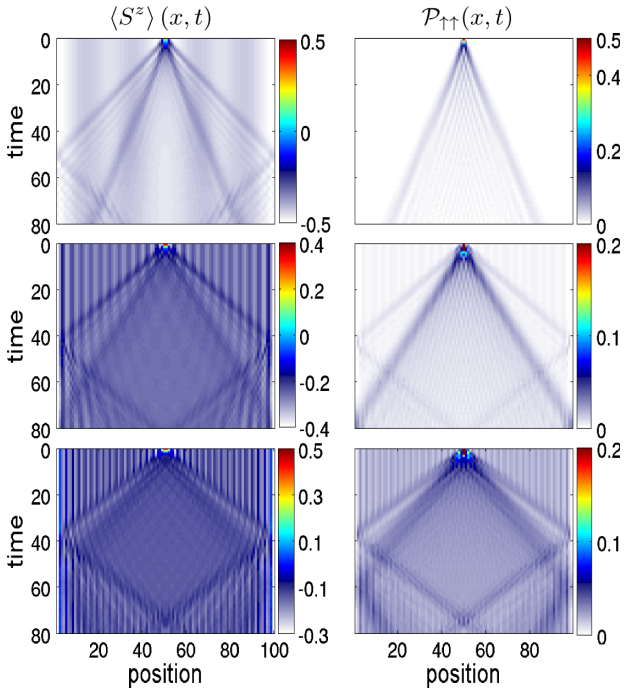

FIG. 2 (color online). 2-string propagation at finite magnetization per site m at $\Delta = 1.2$, corresponding to the Luttinger liquid phase of the model. From top to bottom, $m = -0.44$, $m = -0.26$, and $m = -0.14$. The initial state at $t = 0$ is the ground state of (1) with an infinite magnetic field term at two sites in the center of the chain (chain length $N = 100$). At $t = 0$, the field is switched off and the state is evolved. The striped patterns visible in all plots are Friedel oscillations due to open boundary conditions.

TEBD data are $v_1 \approx 1.26 \pm 0.02$, $v_2 \approx 0.702 \pm 0.025$, and $v_3 \approx 0.370 \pm 0.02$, respectively. These values agree with the maximal velocities of spinons, 2-strings, and 3-strings calculated from the Bethe ansatz, which are $v_{\max} \approx 1.263$, $v_{\max,2} \approx 0.705$, and $v_{\max,3} \approx 0.375$.

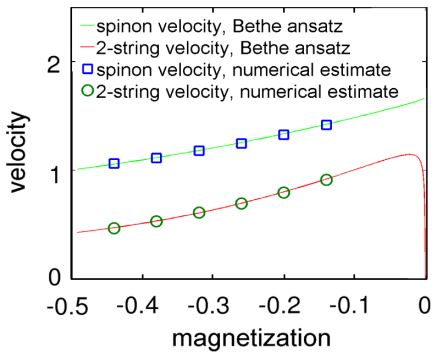

FIG. 3 (color online). Propagation velocity of single-spinon and 2-string branch as a function of total magnetization per site m of the system at $\Delta = 1.2$. Green and red curves show single-spinon and 2-string velocities as calculated from the Bethe ansatz. Green circles and blue squares are numerically derived values from real time simulations. Error bars are smaller than symbols.

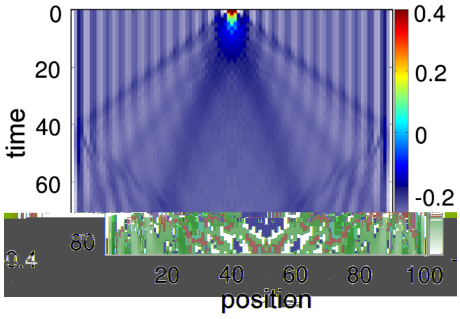

FIG. 4 (color online). Spacetime plot of $\langle S^z \rangle$ for a setup similar to Fig. 2 with $N = 101$ at total magnetization $m = -0.2525$, $\Delta = 1.2$, with three particles at the chain center at $t = 0$.

Integrability-breaking perturbations.—In general, string states are not protected kinematically from decaying into scattering states of spinons. Their stability is then a consequence of integrability of the Heisenberg chain, and an important question is whether signatures of bound states survive when integrability-breaking perturbations are taken into account. In order to address this issue we have considered two types of perturbation: (i) a next-nearest-neighbor interaction and (ii) a spatially varying magnetic field term $\gamma \sum_{j=1}^{N} (j - \frac{N}{2})^2 S_j^z$, which would model an optical trap in certain realizations of (1) based on cold fermionic atoms. In both cases we observe signatures of bound states, indicating that they survive in the form of resonances. We show results for case (i) in Fig. 5.

Conclusions.—We have studied local quantum quenches in the antiferromagnetic spin-1/2 Heisenberg XXZ chain. We observed that above certain thresholds in the interaction strength Δ local observables exhibit prominent signatures associated with linearly propagating gapped bound states. Given the difficulty in observing these bound states in scattering experiments on quantum magnets [10,12], we propose that nonequilibrium setups of the kind considered here are an ideal setting for observing them and probing their properties. Heisenberg spin chains can, e.g., be realized experimentally in crystals and systems of cold atoms in optical lattices with time and space resolved dynamics [20,21]. Recent work has focused on ac driven optical lattices [22] and two-component Bose mixtures [23]. The kind of local perturbation characterizing our initial state could be induced by a focused laser beam.

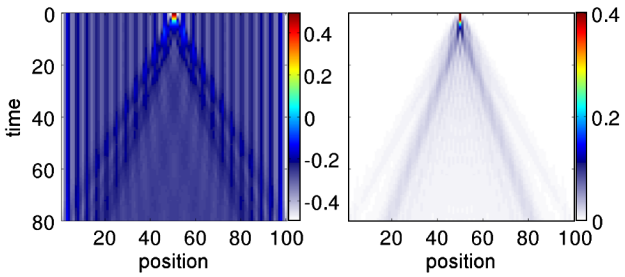

FIG. 5 (color online). Spacetime plot of $\langle S^z \rangle$ and $P_{\uparrow\uparrow}$ for $N = 100$, $m_0 = 2$ at total magnetization $m = -0.26$, $\Delta = 1.2$ and an extra integrability-breaking term $(J/10)\sum_j \mathbf{S}_j \cdot \mathbf{S}_{j+2}$ added to $H(\Delta, B_0)$. Bound state signatures are seen to persist.

We thank P. Calabrese, J. Cardy, and A. Silva for helpful comments and discussions. This work was supported by the Austrian Science Fund (FWF) within the SFB ViCoM (F41) and by the EPSRC under Grant No. EP/I032487/1. F. H. L. E. and H. G. E. thank the KITP for hospitality. This research was supported in part by the NSF under Grant No. NSF PHY05-51164.

*evertz@tugraz.at

[1] M. Greiner, O. Mandel, T. W. Hänsch, and I. Bloch, Nature (London) **419**, 51 (2002); S. Hofferberth, I. Lesanovsky, B. Fischer, T. Schumm, and J. Schmiedmayer, Nature (London) **449**, 324 (2007); S. Trotzky, Y.-A. Chen, A. Flesch, I. McCulloch, U. Schollwöck, J. Eisert, and I. Bloch, arXiv:1101.2659.

[2] T. Kinoshita, T. Wenger, and D. S. Weiss, Nature (London) **440**, 900 (2006).

[3] J. Dziarmaga, Adv. Phys. **59**, 1063 (2010); A. Polkovnikov, K Sengupta, A. Silva, and M. Vengalattore, Rev. Mod. Phys. **83**, 863 (2011); A. Lamacraft and J. E. Moore, arXiv:1106.3567.

[4] M. Rigol, V. Dunjko, V. Yurovsky, and M. Olshanii, Phys. Rev. Lett. **98**, 050405 (2007); M. Rigol, V. Dunjko, and M. Olshanii, Nature (London) **452**, 854 (2008); P. Calabrese and J. Cardy, Phys. Rev. Lett. **96**, 136801 (2006); J. Stat. Mech. (2007) P06008; (2005) P04010; M. A. Cazalilla, Phys. Rev. Lett. **97**, 156403 (2006); S. R. Manmana, S. Wessel, R. M. Noack, and A. Muramatsu, Phys. Rev. Lett. **98**, 210405 (2007); M. Cramer, C. M. Dawson, J. Eisert, and T. J. Osborne, Phys. Rev. Lett. **100**, 030602 (2008); T. Barthel and U. Schollwöck, Phys. Rev. Lett. **100**, 100601 (2008); G. Roux, Phys. Rev. A **79**, 021608 (2009); D. Fioretto and G. Mussardo, New J. Phys. **12**, 055015 (2010); C. Kollath, A. M. Läuchli, and E. Altman, Phys. Rev. Lett. **98**, 180601 (2007); G. Biroli, C. Kollath, and A. M. Läuchli, Phys. Rev. Lett. **105**, 250401 (2010); D. Rossini, S. Suzuki, G. Mussardo, G. E. Santoro, and A. Silva, Phys. Rev. B **82**, 144302 (2010); P. Calabrese, F. H. L. Essler, and M. Fagotti, Phys. Rev. Lett. **106**, 227203 (2011).

[5] The boundary conditions do not affect the propagation noticeably until the wave front reaches the boundary.

[6] D. B. Abraham, E. Barouch, G. Gallavotti, and A. Martin-Löf, Phys. Rev. Lett. **25**, 1449 (1970); Stud. Appl. Math. **50**, 121 (1971).

[7] G. Vidal, Phys. Rev. Lett. **91**, 147902 (2003); **93**, 040502 (2004).

[8] A. J. Daley, C. Kollath, U. Schollwöck, and G. Vidal, J. Stat. Mech. (2004) P04005; S. R. White and A. E. Feiguin, Phys. Rev. Lett. **93**, 076401 (2004).

[9] D. Gobert, C. Kollath, U. Schollwöck, and G. Schütz, Phys. Rev. E **71**, 036102 (2005); D. Petrosyan, B. Schmidt, J. R. Anglin, and M. Fleischhauer, Phys. Rev. A **76**, 033606 (2007); **77**, 039908(E) (2008); S. Langer, F. Heidrich-Meisner, J. Gemmer, I. P. McCulloch, and U.

Schollwöck, Phys. Rev. B **79**, 214409 (2009); J. Ren and S. Zhu, Phys. Rev. A **81**, 014302 (2010); L. F. Santos and A. Mitra, Phys. Rev. E **84**, 016206 (2011); R. Steinigeweg, S. Langer, F. Heidrich-Meisner, I. P. McCulloch, and W. Brenig, Phys. Rev. Lett. **106**, 160602 (2011); S. Langer, M. Heyl, I. P. McCulloch, and F. Heidrich-Meisner, Phys. Rev. B **84**, 205115 (2011).

[10] R. G. Pereira, S. R. White, and I. Affleck, Phys. Rev. Lett. **100**, 027206 (2008).

[11] P. Calabrese and J. Cardy, J. Stat. Mech. (2007) P10004; J. M. Stéphan and J. Dubail, J. Stat. Mech. (2011) P08019.

[12] J.-S. Caux and J.-M. Maillet, Phys. Rev. Lett. **95**, 077201 (2005); J.-S. Caux, R. Hagemans, and J.-M. Maillet, J. Stat. Mech. (2005) P09003; R. G. Pereira, S. R. White, and I. Affleck, Phys. Rev. B **79**, 165113 (2009); M. Kohno, Phys. Rev. Lett. **102**, 037203 (2009); A. Shashi, L. I. Glazman, J.-S. Caux, and A. Imambekov, Phys. Rev. B **84**, 045408 (2011); A. Imambekov, T. L. Schmidt, and L. I. Glazman, arXiv:1110.1374.

[13] M. Takahashi and M. Suzuki, Prog. Theor. Phys. **48**, 2187 (1972); M. Fowler and X. Zotos, Phys. Rev. B **24**, 2634 (1981).

[14] B. Sutherland, *Beautiful Models* (World Scientific, Singapore, 2004).

[15] E. H. Lieb and D. W. Robinson, Commun. Math. Phys. **28**, 251 (1972).

[16] We note that these wave fronts, while evident in Fig. 1, are not easy to discern in equal time or space slices due to the oscillatory nature of the signal.

[17] I. Affleck and A. Ludwig, J. Phys. A **27**, 5375 (1994).

[18] J. L. Cardy, Nucl. Phys. **B324**, 581 (1989).

[19] S. R. White, Phys. Rev. Lett. **69**, 2863 (1992); Phys. Rev. B **48**, 10 345 (1993).

[20] C. Ramanathan, P. Cappellaro, L. Viola, and D. G. Cory, New J. Phys. **13**, 103015 (2011).

[21] C. Weitenberg *et al.*, Nature (London) **471**, 319 (2011); J. Simon *et al.*, Nature (London) **472**, 307 (2011); M. Cheneau *et al.*, arXiv:1111.0776.

[22] Y.-A. Chen *et al.*, Phys. Rev. Lett. **107**, 210405 (2011).

[23] A. B. Kuklov and B. V. Svistunov, Phys. Rev. Lett. **90**, 100401 (2003); L.-M. Duan, E. Demler, and M. D. Lukin, Phys. Rev. Lett. **91**, 090402 (2003); G. Thalhammer *et al.*, Phys. Rev. Lett. **100**, 210402 (2008).